

**UNIVERSIDAD SAN FRANCISCO DE QUITO USFQ**

**Colegio de Ciencias e Ingenierías**

**Acoustic Standing Waves Modelling in Gas Solid Fluidized  
Beds**

**Proyecto de Investigación**

**Gabriel Guillermo Iturralde Dueñas**

**Ingeniería Mecánica**

Trabajo de titulación presentado como requisito  
para la obtención del título de  
Ingeniero Mecánico

Quito, 11 de mayo de 2016

UNIVERSIDAD SAN FRANCISCO DE QUITO USFQ  
COLEGIO DE CIENCIAS E INGENIERÍAS

**HOJA DE CALIFICACIÓN  
DE TRABAJO DE TITULACIÓN**

**Acoustic Standing Waves Modeling in Gas Solid Fluidized Beds**

**Gabriel Guillermo Iturralde Dueñas**

Calificación:

Nombre del profesor, Título académico

---

David Escudero, PhD

Firma del profesor

---

Quito, 16 de mayo de 2016

## Derechos de Autor

Por medio del presente documento certifico que he leído todas las Políticas y Manuales de la Universidad San Francisco de Quito USFQ, incluyendo la Política de Propiedad Intelectual USFQ, y estoy de acuerdo con su contenido, por lo que los derechos de propiedad intelectual del presente trabajo quedan sujetos a lo dispuesto en esas Políticas.

Asimismo, autorizo a la USFQ para que realice la digitalización y publicación de este trabajo en el repositorio virtual, de conformidad a lo dispuesto en el Art. 144 de la Ley Orgánica de Educación Superior.

Firma del estudiante: \_\_\_\_\_

Nombres y apellidos: Gabriel Guillermo Iturralde Dueñas

Código: 107168

Cédula de Identidad: 1721355939

Lugar y fecha: Quito, 11 de mayo de 2016

## RESUMEN

Los reactores de lecho fluidizado son ampliamente utilizados en aplicaciones industriales debido a su alta transferencia de calor, pequeñas caídas de presión y porque pueden trabajar con una extensa distribución de tamaños de partículas. Las vibraciones acústicas incrementan la calidad de fluidización de manera considerable, por lo cual el entender el comportamiento de este tipo de ondas es de particular interés. Se desarrolló un modelo unidimensional de onda acústica estacionaria para un reactor de lecho de flujo frío de 9.6 cm de diámetro interno relleno con esferas de vidrio con un rango de diámetro de 300-600  $\mu\text{m}$  y cáscara de nuez con un diámetro de partícula entre 600-1000  $\mu\text{m}$ . Se utilizó frecuencias de 80, 100, 150 y 200 Hz, manteniendo un nivel de presión de sonido de la fuente constante de 110 dB. El modelo muestra un buen ajuste tanto para un reactor vacío como para uno relleno con material. Cuando las partículas sólidas son añadidas al reactor se produce un efecto de atenuación.

*Palabras clave:* interacción acústica, ondas acústicas estacionarias, reactor de lecho, velocidad mínima de fluidización, atenuación acústica.

## ABSTRACT

Fluidized beds are extensively used in industrial applications because of their high heat transfer rate, low pressure drops and because they work with a wide range of particle size distributions. Acoustic vibrations increase the fluidization quality in a remarkable way, so understanding the wave pattern that produce this effect is of particular interest. A one dimensional acoustic standing wave model was developed for a 9.6 cm internal diameter cold flow fluidized bed reactor filled with glass beads (300-600  $\mu\text{m}$ ) and ground walnut shell (600-1000  $\mu\text{m}$ ) particles for 80, 100, 150 and 200 Hz sound frequency while keeping the source sound pressure level amplitude constant at 110 dB. The model exhibits a good agreement for an empty reactor and for a filled fluidized bed. When solid particles are added an attenuation effect is produced.

*Key words:* Acoustic field, acoustic standing wave, fluidized bed, minimum fluidization velocity, acoustic attenuation.

## TABLE OF CONTENTS

<b>INTRODUCTION.....</b>	<b>8</b>
<b>CHAPTER 1: METHODS AND EXPERIMENTAL SETUP .....</b>	<b>11</b>
<b>1.1 Acoustic standing wave theory .....</b>	<b>11</b>
<b>1.2 Acoustic attenuation.....</b>	<b>15</b>
<b>1.3 Attenuation coefficient and sound speed for solid material .....</b>	<b>16</b>
<b>1.4 Experimental setup .....</b>	<b>17</b>
<b>CHAPTER 2: RESULTS AND DISCUSSIONS .....</b>	<b>21</b>
<b>2.1 Experimental results .....</b>	<b>21</b>
<b>2.2 Comparison between model and experimental results: .....</b>	<b>23</b>
<b>CONCLUSION.....</b>	<b>26</b>
<b>References .....</b>	<b>27</b>
<b>Appendix A: Sound Pressure Level Definition.....</b>	<b>29</b>

## LIST OF FIGURES

<b>Figure 1:</b> Schematic of the sound wave propagation in a fluidized bed. Source: (Escudero, 2014).....	12
<b>Figure 2:</b> Sound pressure level distribution for different values of $kh$ as function of distance from the distributor plate .....	14
<b>Figure 3:</b> Standing wave comparison with $P_{min}$ and $P_{max}$ lines as function of distance from distributor plate.....	16
<b>Figure 4:</b> Schematic of the fluidized bed reactor (not to scale) .....	19
<b>Figure 5:</b> Sound pressure level as a function of distance from the distributor plate for an empty reactor .....	21
<b>Figure 6:</b> Sound pressure level as a function of distance for a fluidized bed filled with .....	22
<b>Figure 7:</b> Sound pressure level as a function of distance for a fluidized bed filled with .....	23
<b>Figure 8:</b> Experimental and model data for sound pressure level as a function of distance from the distributor plate for an empty reactor.....	24
<b>Figure 9:</b> Experimental and model data for sound pressure level as a function of distance for 300-600 $\mu\text{m}$ glass beads fluidized bed .....	25

## INTRODUCTION

Fluidized beds are reactors in which fluidization of solid particles takes place. Fluidization occurs when the drag force produced by an upward-flowing gas is high enough to overcome the force of gravity, giving the solid particles a fluid-like behavior. They are widely used in chemical reactions (i.e. about 75% of all polyolefins are produced by this method), pharmaceutical applications, oil shale retorting processes, food industries and in advanced material technology. They provide three main advantages from the other fluidization techniques: considerably high heat transfer rate, capability to easily move solids like a fluid and to have a wide range of particle size distribution. (Cocco et.al, 2014) For a gas-solid system, which is the case of this study, their industrial applications are classified in four categories (Crowe & Michaelides, 2006): gas catalytic reactions, gas phase reactions using solids as heat carriers, gas solid reactions and in processes where no chemical reaction occur such as in bed drying procedures.

In addition, the minimum fluidization velocity ( $U_{mf}$ ) is one of the most relevant normalized parameter in describing the hydrodynamics of a fluidized bed (Ramos Caicedo et al, 2002). It is defined as the superficial gas velocity at which the drag force of the particles equals the weight of the particles in the fluidizing medium and theoretically is given by Ergun equation (Cocco et al., 2014). The minimum fluidization velocity depends on material properties, bed geometry and fluid properties (Guo et.al, 2011, Ramos Caicedo et al, 2002, Gunn & Hilal, 1997) For this study, the minimum fluidization velocity used values are the ones determined by Escudero and Heindel (Escudero & Heindel, 2013).

Granular material is classified using a Geldart chart, which relates the density of the particle with the particle diameter (Geldart, 1973). Fine Geldart B powders (ranging between 150-1000  $\mu\text{m}$ ) are commonly difficult to fluidize due to the strong interparticle and cohesive forces. They adhere to each other by agglomerating attractions, due to liquid surface tension between particles, and van der Waals forces that are related with the local electric field between molecules. In the last few decades, several scientific articles have shown results that prove that acoustic waves improve drastically the fluidization of this type of powders, reducing minimum fluidization velocity and channeling (i.e. formation of a channel of fast passing bubbles across the bed). (Guo, Liu et al 2006; Levy et al 1997; Russo, 1995). This is particularly interesting, because there are not internal changes generated inside the bed and there are no restrictions on which particle type can be fluidized.

Previous investigations have reported that at low frequencies and high sound pressure levels Geldart A and C particles increase their fluidization behavior. Guo et al. studied the influence of sound frequency and sound pressure level on fluidization patterns with micron and nanoparticles by measuring bed pressure drop and minimum fluidization velocity (Guo et al., 2006). The results showed that at a frequency range of 40-70 Hz and sound pressure greater than 100 dB, stable fluidization was reached. In addition, at constant frequency while increasing sound pressure level, fluidization quality improved significantly despite of a decrease on minimum fluidization velocity.

Furthermore, Russo et al. reported a significant improvement in fluidization quality at a frequency range of 110 to 140 Hz using 0.5-45 $\mu$ m catalyst particles with a total mass combination up to 3 kg and sound pressure level varying from 110 to 140 dB, through observing the breakup of original clusters into subclusters. This phenomenon is attained when drag and inertial forces (external loads) exceed the internal forces given by van der Waals and other cohesive attractions. A ratio of presence of clusters and subclusters obtained was 1.5-3 (Russo et al., 1995). In addition, they developed a cluster to subcluster oscillatory model that evidenced the mistaken hypothesis of rigid bed structures. This is an important assumption made in this article.

Guo, et al. studied the effect of temperature, sound wave frequency and sound pressure level for quartz and silica particles. (Guo, Zhang, & Hao, 2011). The same results as Russo et al, Guo et al. for the effect of sound pressure level and frequency were obtained in the fluidizing behavior inside the bed. However, they reached to the conclusion that minimum fluidization velocity decreases with increasing temperature. One interesting consideration of their analysis was that there exists a minimum value of the minimum fluidization velocity corresponding to good fluidization quality that is related with the natural frequency of the gas solid system.

In addition, Xu et al. determined that for a 100 mm internal diameter and 1000 mm bed height using fine powder ranging from 4.8-65  $\mu$ m, exists a resonant frequency ranging between 100 to 110 Hz in which the effectiveness of the sound wave improves remarkably the fluidization of this type of particulate solids (Xu, Cheng, & Zhu, 2006). Moreover, they studied how the fluidization indicators vary considerably with the size of the Geldart type particles due to their attenuation coefficients.

Herrera et al. used one open and one closed ends system to establish the characteristics of acoustic standing waves (Herrera, Levy, & Ochs, 2002). A 1D, quasi fluid with constant speed of sound model applying acoustic wave theory was applied for the sound pressure level

distribution. They determined that an important resonant bed depth depends on the bed height and a parameter  $k$  called the wave number that is proportional to the sound wave frequency and inversely proportional to the sound speed in the medium. The natural frequency of the systems was obtained and is the frequency at which the highest sound pressure level occurs.

Further studies were done by Shuai et al. in which they applied CFD methods in a 2D fluidized bed simulating cohesive and fluid forces for large diameters of Geldart particles. (Shuai et al, 2010). The results achieved showed good agreement with the real fluidizing behavior. They concluded that there is a range of sound frequencies between 100-120 Hz at a sound pressure level of 120 dB in which the cohesive forces reaches minimum and the acoustic and contact forces are maximum.

However, the applicability of this models have not been studied yet for different heights of Geldart B particles ranging between 300-1000  $\mu\text{m}$  such as ground walnut shell and glass beads.

It is remarkably important in determining the influence of standing acoustic waves in the fluidization quality of beds, to analyze the characterization of the acoustic waves that generate this phenomenon. This main properties of acoustic waves that originates this situation are amplitude, natural frequency, attenuation coefficient and wave shape.

In this investigation, a 1D standing acoustic wave model based on Herrera et al.'s model (Herrera et al., 2002) will be used for ground walnut shell and glass beads in order to determine its applicability for this type of gas solid system. The aim is to understand more deeply the behavior of sound wave inside the fluidized bed for Geldart B particles under different conditions of frequency, minimum fluidization velocity while keeping constant the amplitude of sound pressure level at ambient temperature.

# CHAPTER 1: METHODS AND EXPERIMENTAL SETUP

## 1.1 Acoustic standing wave theory

When longitudinal waves travel through a fluid they are referred as acoustic waves. When a medium (i.e. a gas solid system) is dynamically disturbed, a momentum is imparted and transmitted to adjacent particles that are set into motion due the collisions between them. The amplitude of this oscillations is called sound pressure that is defined as the change in pressure from the static pressure in the fluid in which the wave propagates. (Reynolds, 1988). This disturbance modifies also the particle velocity, fluid density and temperature. Furthermore, for one dimensional and adiabatic wave propagation, the wave equation written in terms of pressure is given by (Reynolds, 1988):

$$\frac{\partial^2 p}{\partial x^2} = \frac{1}{c^2} \frac{\partial^2 p}{\partial t^2} \quad (1)$$

Where  $p$  is the sound pressure,  $x$  is distance along the axis of wave motion,  $t$  is the time and  $c$  is the speed of sound in the medium. This expression has a solution of the form:

$$p(x, t) = Ae^{-j(\omega t - kx)} \quad (2)$$

Where  $k$  is the wave number, defined as  $k = \omega/c$  or in terms of frequency,  $k = 2\pi f/c$ ;  $\omega$  is the angular frequency and  $A$  is a constant that depends of boundary conditions.

In addition, for a fluidized bed with two single-phase (gas and solid) elements with one rigid boundary and an open end, sound waves are transmitted in the following way: an incident wave pressure coming from the acoustic source ( $P_i$ ) travels through the air, when  $P_i$  reaches the interface between air and the fluidizing material, part of the oscillation energy is transmitted downward to the particulate material ( $P_t$ ) and the other is reflected ( $P_r$ ) back to the empty region of the bed. Once the incident wave ( $P_{i1}$ ) reaches the distributor plate, another part of the wave energy is reflected ( $P_{r1}$ ). This produces an additive effect referred as “standing wave”

(Kinsler et al, 1962). In figure 1, is shown a schematic of the way acoustic waves are propagated across a gas-solid fluidized bed:

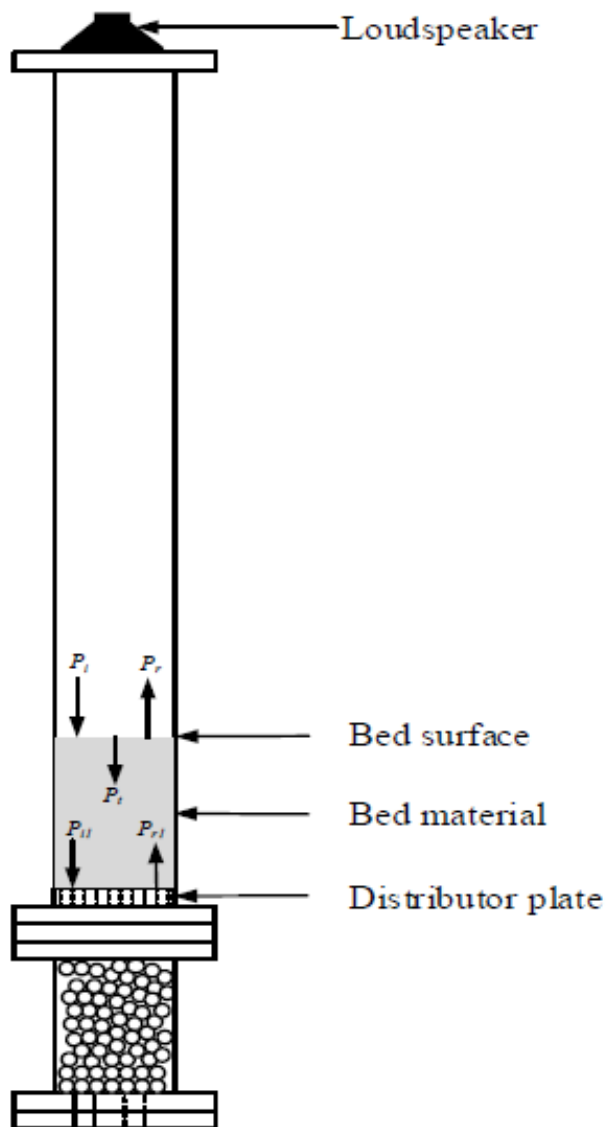


**Figure 1:** Schematic of the sound wave propagation in a fluidized bed. Source: (Escudero, 2014)

The ratio of the transmitted and reflected portions of the incident wave depends on the acoustic impedance of the medium. For equal impedance, all energy is transmitted downward. (Herrera et al, 2002).

Applying standing wave theory, a simple 1D model of the transmission of acoustic wave across the fluidized bed was developed. In this study, the model equations were developed in Matlab and were based on the previous model developed by Herrera et al. (Herrera et al., 2002).

The sound pressure distribution is described by the following equation:

$$p(x, t) = P_{fs} \sqrt{\frac{\cos^2 kx}{\cos^2 kh}} \cos \omega t \quad (3)$$

where  $P_{fs}$  is source amplitude,  $k$  is the wave number described above and  $h$  is the height of the static bed material inside the fluidized bed.

The boundary condition of the case of this study is set at the open end ( $x=h$ ), where the loudspeaker is located, in which the pressure becomes:

$$p(x, h) = P_{fs} \cos \omega t \quad (4)$$

The amplitude of Eq. 3, considering that it is an even function, is:

$$|p(x, t)| = P_{fs} \sqrt{\frac{\cos^2 kx}{\cos^2 kh}} \quad (5)$$

Sound pressure is commonly expressed in units of decibels and it is known as sound pressure level (SPL). See the appendix for the conversion from sound pressure to SPL (dB).

Furthermore, the resonant state and minimum points (nodes) of this model occurs when:

$$kh = (2n - 1) \frac{\pi}{2} \quad \text{for } n=1,2, \dots \quad (6)$$

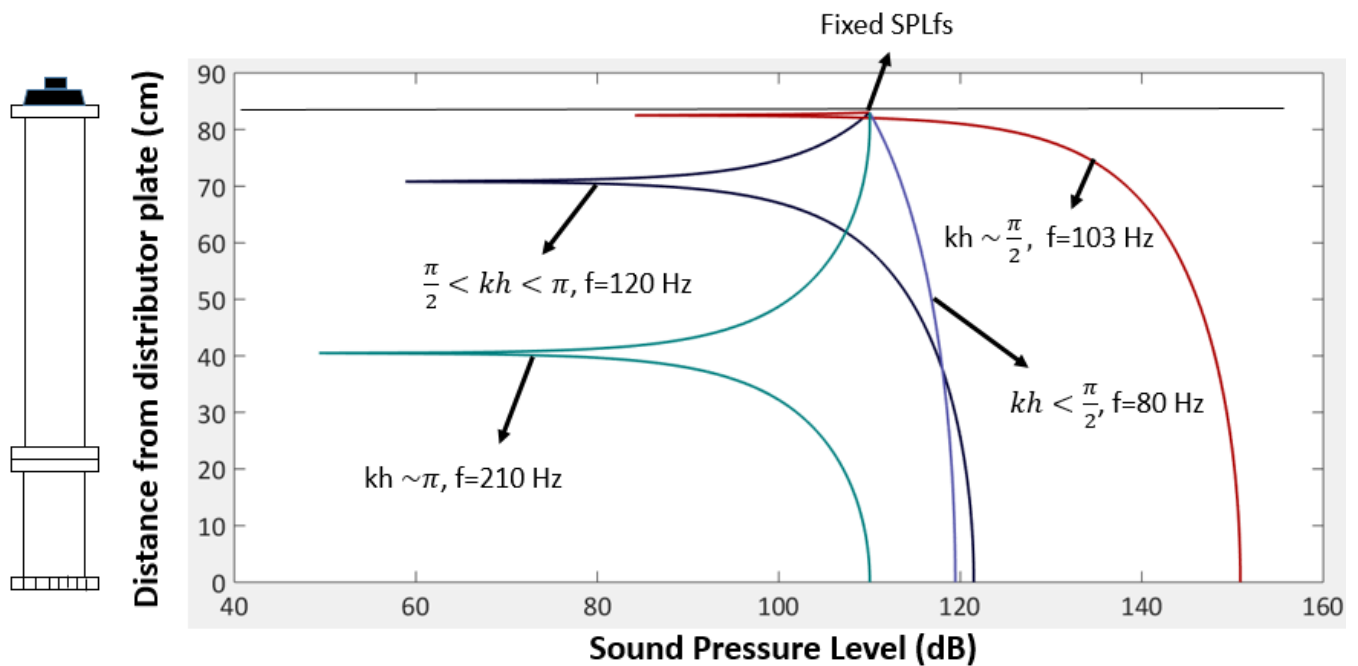
This is of particular interest due higher pressure level increases fluidization quality.

Figure 2 shows the sound pressure level distribution for different values of  $kh$ , by changing the frequency of the acoustic wave.

One additional parameter of particular interest is the bed reactor natural frequency because at this point better fluidizing quality is achieved. It can be obtained through the following equation (Kaliyaperumal, Barghi, Zhu, Briens, & Rohani, 2011):

$$f = \frac{1}{4L} \sqrt{\frac{RT\rho_g}{\varepsilon(1-\varepsilon)\rho_p}} \quad (7)$$

where  $L$  is the bed height,  $T$  is the temperature in SI units,  $\varepsilon$  is the voidage coefficient (defined as the ratio between the particle density and the particle bulk density),  $\rho_p$  is the particle density,  $\rho_g$  is the gas density at the specified temperature and  $R$  is the gas constant of the medium.



**Figure 2:** Sound pressure level distribution for different values of  $kh$  as function of distance from the distributor plate

## 1.2 Acoustic attenuation

Attenuation is an acoustic property of the medium that depends on the sound wave frequency. This phenomenon can be originated due to viscous losses, heat conduction losses and losses associated with internal molecular processes. (Kinsler et al, 1962). Viscous dissipation is produced by the relative motion between adjacent particles (which is mainly the source of attenuation of this case of study). Moreover, heat conduction losses are formed from the conduction of thermal energy from a temperature differential between condensation and rarefactions. Molecular process of absorption include conversion of kinetic energy in stored energy, as it happens in clusters (which is relevant for this research) and into rotational and vibrational energy.

All this contributions are added into a general attenuation coefficient that can be obtained by a theoretical equation (classical approach) or tabulated in plots or tables according to the sound frequency. (Kinsler et al, 1962; Reynolds, 1988).

The attenuation effect can be added to the sound pressure amplitude distribution as follows (Herrera et al., 2002):

$$|p(x, t)| = 2A\sqrt{\cosh^2\alpha x \cos^2 kx + \sinh^2\alpha x \sin^2 kx} \quad (8)$$

where  $\alpha$  is the attenuation coefficient in 1/m units and A is a constant that depends on boundary conditions.

Applying the same boundary condition of Eq 4, the following expression is obtained:

$$|p(x, t)| = Pfs \sqrt{\frac{\cosh^2\alpha x \cos^2 kx + \sinh^2\alpha x \sin^2 kx}{\cosh^2\alpha h \cos^2 kh + \sinh^2\alpha h \sin^2 kh}} \quad (9)$$

The nodal points of minimum pressure can be detected at (Herrera et al., 2002):

$$kx = (2n - 1)\frac{\pi}{2} \quad \text{for } n=1, 2, \dots \quad (10)$$

Thus, the minimum pressure at that points is (Herrera et al., 2002):

$$P_{min} = 2A \sinh(\alpha x) \quad \text{for } n=1,2, \dots \quad (11)$$

In addition, the nodal points of maximum pressure are expressed by (Herrera et al., 2002):

$$kx = n\pi \quad \text{for } n=0, 1, 2, \dots \quad (12)$$

Thus, the maximum pressure becomes (Herrera et al., 2002):

$$P_{max} = 2A \cosh(\alpha x) \quad (13)$$

Figure 3 presents a schematic of the effect of attenuation on a sound wave at frequency of 520 [Hz] and an attenuation coefficient of 0.3 [1/m] taken from Kinsler et al. (Kinsler et al. 1962). The lines of minimum and maximum pressure are also shown.

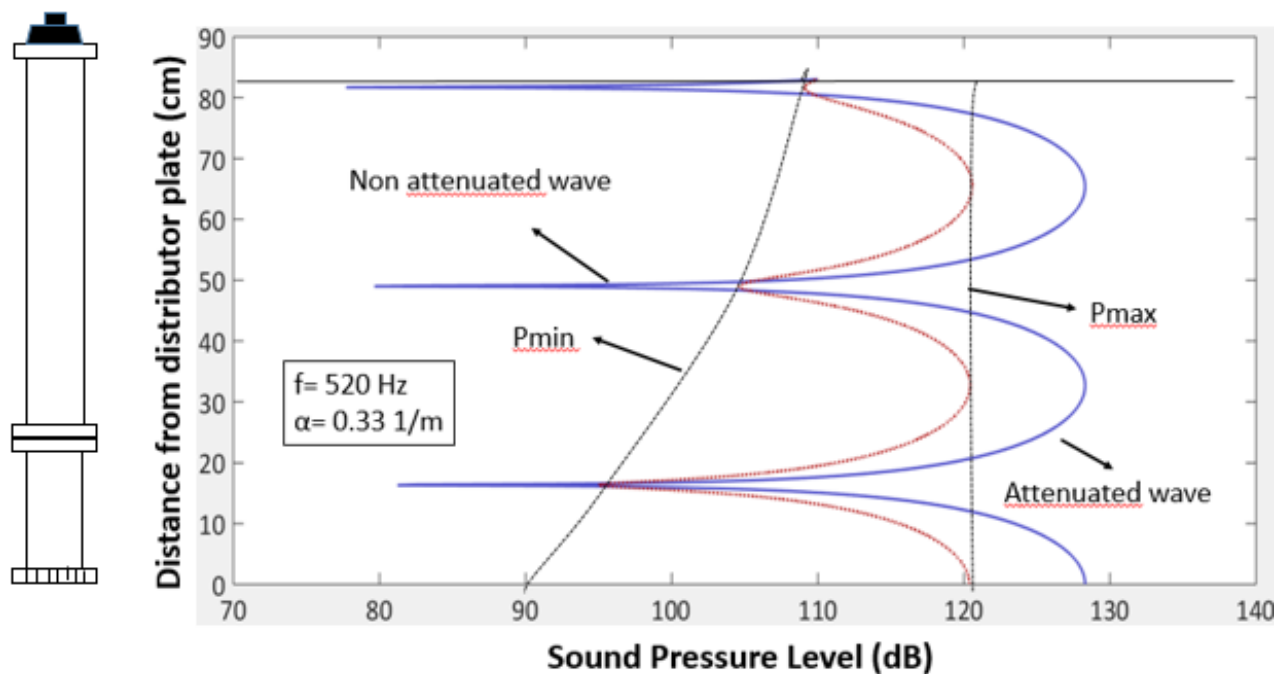


**Figure 3:** Standing wave comparison with Pmin and Pmax lines as function of distance from distributor plate

### 1.3 Attenuation coefficient and sound speed for solid material

Shuai et al. reached to a theoretical equation to obtain the attenuation coefficient produced by a gas solid medium, that is a function of the sound frequency and sound velocity in air (Shuai et al., 2011):

$$\alpha = \frac{2b(\pi f)^2}{(\varepsilon_s \rho_s + \varepsilon_g \rho_g) c_o^3} \quad (14)$$

Where  $b$  is the dynamic air viscosity at ambient temperature and is equal to  $10^{-5}$  [ $\text{kg m}^{-1} \text{s}^{-1}$ ],  $f$  is the frequency,  $\varepsilon_s$  a factor of concentration of particles defined as the ratio of the bulk and particle density of the solid material,  $\rho_s$  is the particle density,  $\rho_g$  is the gas density,  $\varepsilon_g$  is the porosity expressed as  $1-\varepsilon_s$ , and  $c_o$  that is the air speed at ambient temperature and atmospheric pressure (340 [m/s]). This is the classical approach described in last section.

During the development of this study, the attenuation coefficient for the particulate solid will be calculated experimentally, taking the theoretical value of Eq. 13, based on the following relation (Guo et al., 2006) and on Eq. 8:

$$SPL \propto SPL_0 h^{-2} e^{-2\alpha h} \quad (15)$$

Where  $SPL_0$  is the initial sound pressure level and  $SPL$  is the sound pressure level when the sound wave has propagated a distance  $h$  from the distributor plate.

Similarly, once the material is added to the fluidizing bed, the velocity of sound for the gas-solid is defined as (Kaliyaperumal et al, 2011):

$$c = \sqrt{\frac{\left[ \frac{\varepsilon_s}{k_g} + \frac{(1-\varepsilon_s)}{k_s} \right]^{-1}}{\varepsilon_s \rho_g + (1-\varepsilon_s) \rho_p}} \quad (16)$$

where  $c$  is the speed of sound in gas solid media,  $k_g$  is the gas bulk modulus equal to 0.117 MPa,  $k_s$  is the particle gas bulk modulus equal to 40 GPa of the glass beads.

## 1.4 Experimental setup

The experiments were developed in a cold fluidized bed reactor. As shown in Fig 4, it is formed by three main chambers: the top chamber or freeboard region (made of PVC), the bed chamber and the plenum (both were fabricated using a 9.6 cm internal diameter acrylic cylinder with a 0.4 cm wall thickness). Fluidization takes place within the bed chamber which is 22 cm

tall and 9.6 cm internal diameter. The sections are connected through square flanges of 15.8 x 15.8 cm. The distributor plate is made of acrylic with 5 mm diameter holes spaced approximately 8 mm apart in a circular grid with a total of 0.38% total open area.

Compressed air from a compressor is used as the fluidizing gas. The compressor delivers air to the laboratory at 482 kPa (70 psi). The fluidized bed air flow is regulated by a pressure regulator, with a pressure range of 0-117 kPa (0-17 psi). In addition, a ball valve and a flow meter are added to control the superficial gas velocity of the chamber. The flow meter has a flow range of 0-10 cfm.

The fluidizing particles used in this study are glass beads ( $\rho_{glass} = 2500 \text{ kg/m}^3$ ) ranging between 300-600  $\mu\text{m}$  diameter and ground wall shell ( $\rho_{walnut\ shell} = 1440 \text{ kg/m}^3$ ) ranging between 600-800  $\mu\text{m}$  diameter. In order to prepare the material, a series of sieves sizes and a mechanical shaker were utilized. The material was slowly added to the bed chamber until a height equal to the internal diameter size was reached. In figure 4, a schematic of the fluidized bed reactor described above is shown:

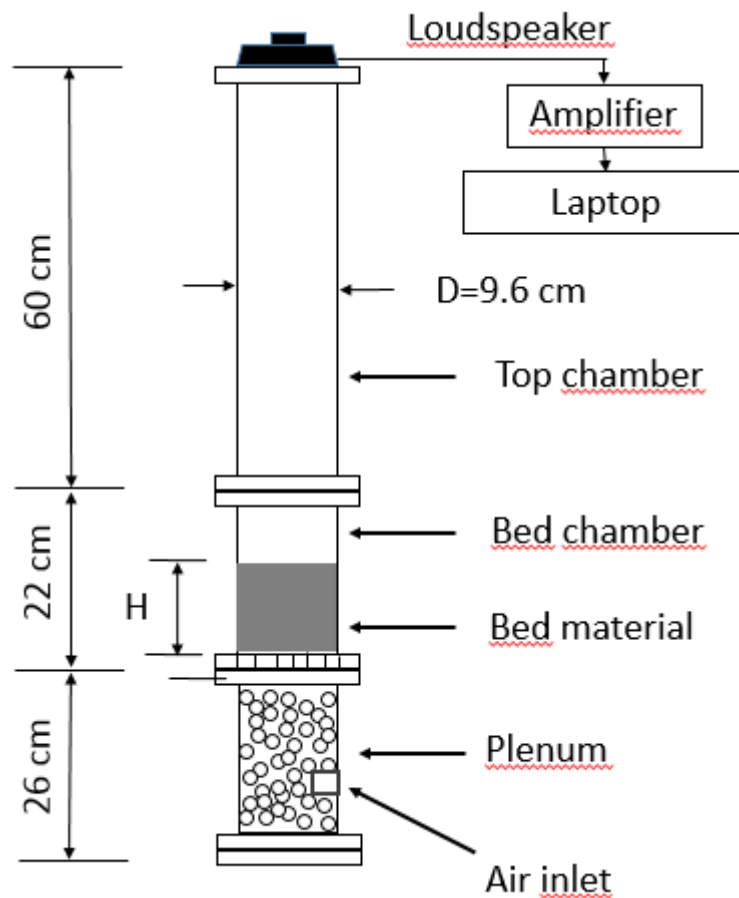


**Figure 4:** Schematic of the fluidized bed reactor (not to scale)

The acoustic waves were generated by a laptop using Room Equalizer Wizard audio analysis software. The sound was amplified by a Radio Shack 40W amplifier to a Peerless loudspeaker with an impedance of 8 ohms. An UMM-6 Dayton Audio Measurement microphone was used to measure the sound pressure level distribution inside the fluidized bed produced from the loudspeaker using a calibration file (which can be downloaded from the fabricant website) on the audio analysis software.

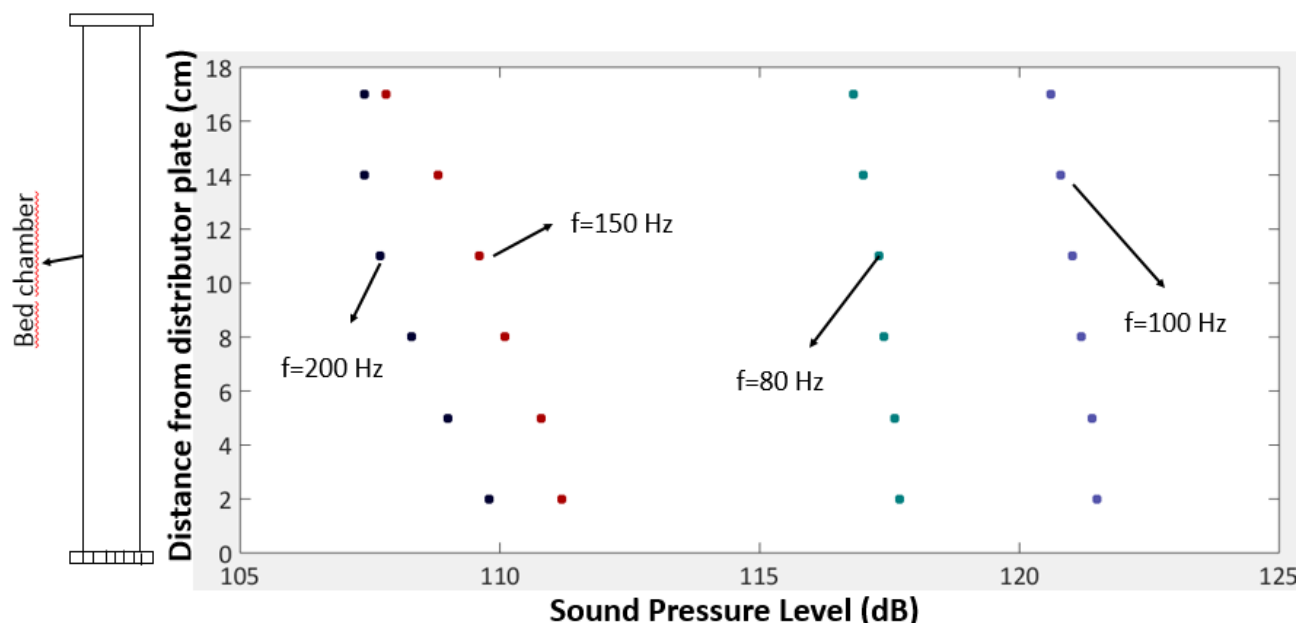
Furthermore, six holes were drilled in the bed chamber at equally spaced positions with a 0.8 cm diameter which corresponds to the external diameter of the microphone. An additional hole was made on the top of the bed at a height close to the loudspeaker in order to set the source sound pressure level. The holes were sealed with bolt depots while they were not operating. In all this locations the sound pressure level was recorded using the mic.

This procedure was performed first with an empty reactor with a constant sound pressure level at the loudspeaker (source) of 110 dB. The sound pressure distributions was recorded for waves of 80, 100, 150 and 200 Hz. The same method was applied for the chamber filled with both materials (glass beads and ground walnut shell). In both situations, 3 different minimum fluidization velocities were used (0 Umf, 1 Umf and 3 Umf) in order to determine the influence of this parameter in the sound pressure level behavior. The minimum fluidization velocity reference values were determined by Escudero and Heindel. (Escudero & Heindel, 2013).

## CHAPTER 2: RESULTS AND DISCUSSIONS

### 2.1. Experimental results

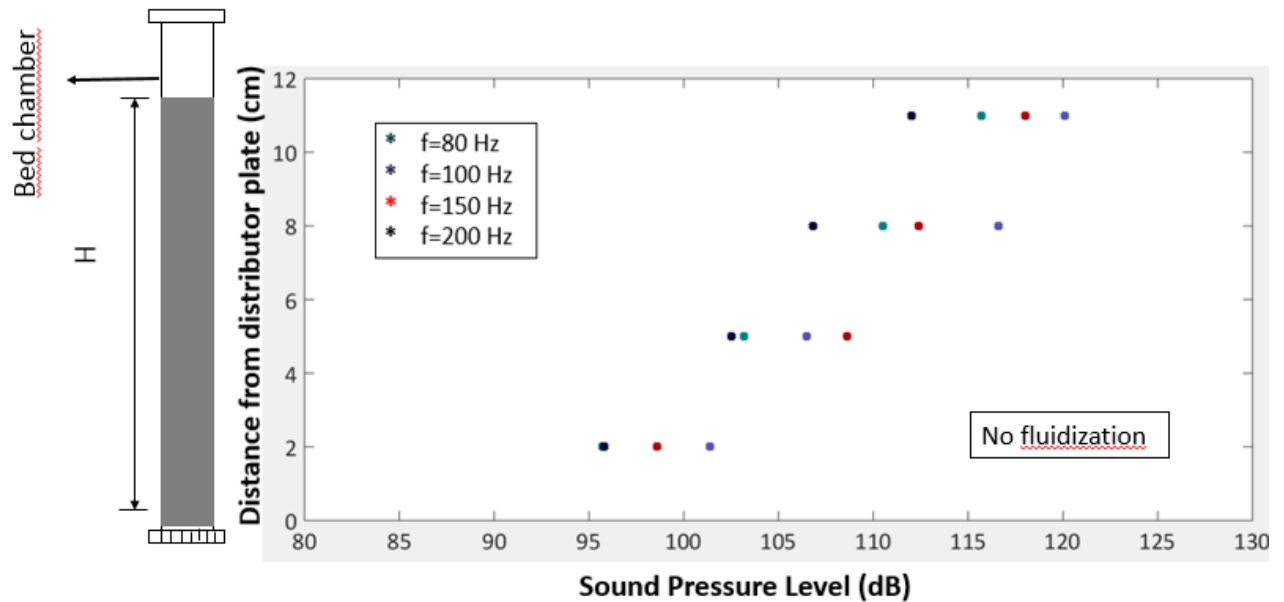
Sound pressure level was measured in six different position along the bed chamber for an empty fluidized bed, and for a bed filled with glass beads and ground walnut shell. A source constant sound pressure level amplitude of 110 dB was set. Figure 5 shows the sound level distribution for an empty reactor at frequencies of 80, 100, 150 and 200 Hz. As it can be seen, as frequency increases the sound pressure level distribution exhibits more tendency of acoustic standing wave behavior. The same results were obtained by Herrera et al. (Herrera et al., 2002)



**Figure 5:** Sound pressure level as a function of distance from the distributor plate for an empty reactor

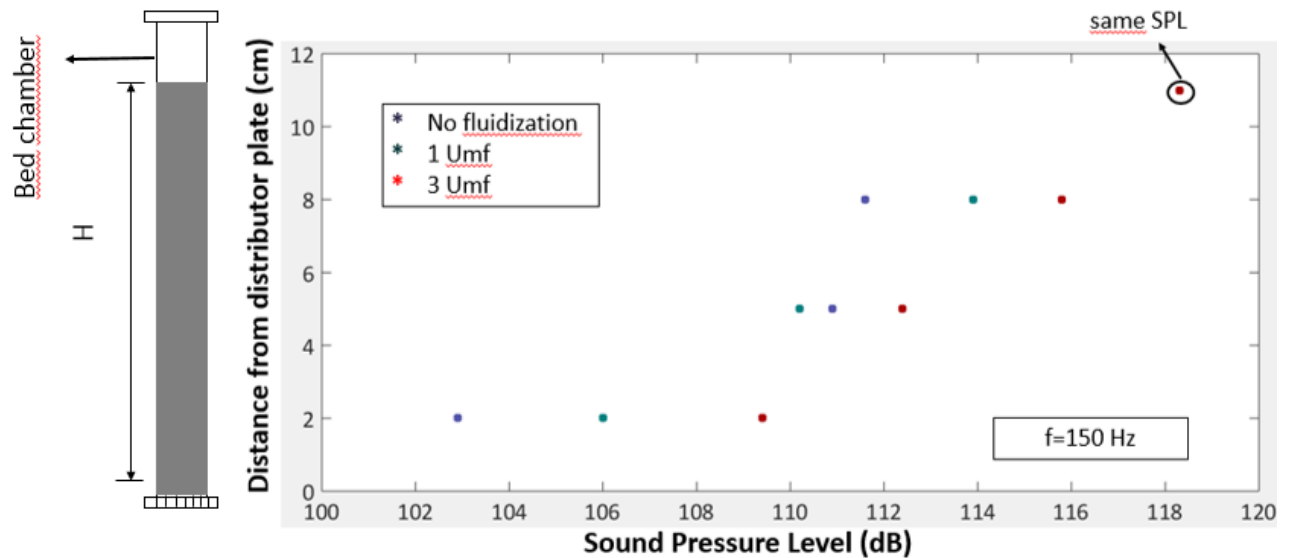
As shown in Fig 6, adding solid particles to the bed chamber modifies the sound pressure profile. Figure 6 shows the sound level pressure distribution as a function of the distance from the distributor plate for a fluidized bed filled with 300-600  $\mu\text{m}$  glass beads to an initial bed height of  $H/D=1$ . As the sound wave emitted from the source reaches the interface with the material part of the energy is transmitted downward and some is reflected. So an effect of

attenuation is achieved showing a decrease in the sound intensity, which depends on the material properties and in the sound frequency, in comparison with the ones in the empty reactor as the acoustic wave propagates deeper.



**Figure 6:** Sound pressure level as a function of distance for a fluidized bed filled with 300-600  $\mu\text{m}$

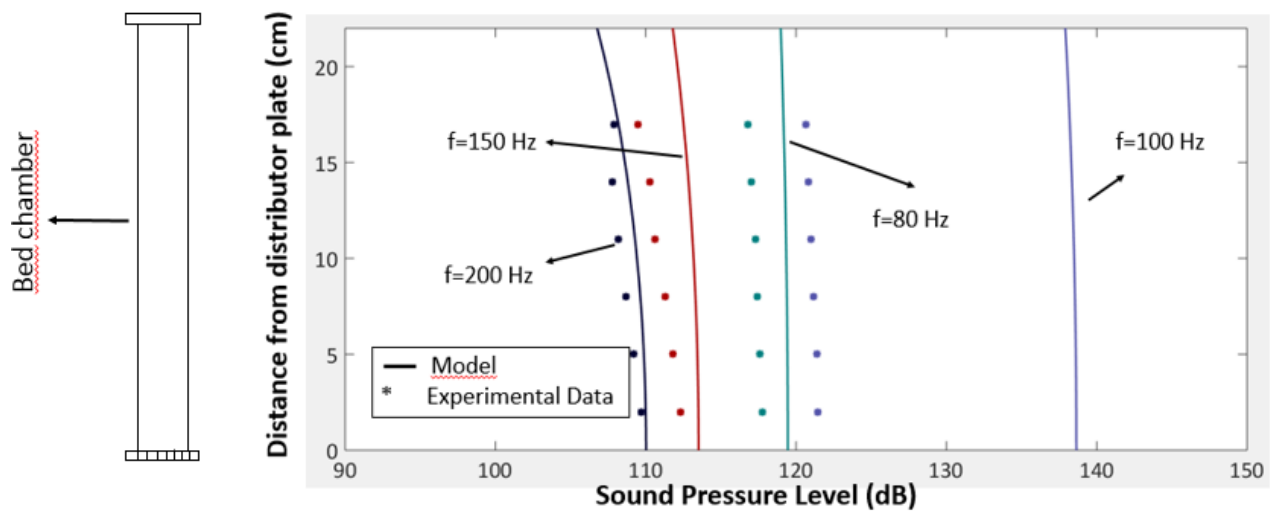
In addition, in Fig 7 the effect of increasing the superficial gas velocity for a bed filled with ground walnut shell is shown. Figure 7 presents the sound pressure level profile as a function of the distance from the distributor plate for a reactor filled with 600-1000  $\mu\text{m}$  ground walnut shell for different values of minimum fluidization velocity (0  $U_{mf}$ , 1  $U_{mf}$  and 3  $U_{mf}$ ) for a frequency of 150 Hz. As it can be observed, there is slight change in the sound intensity of (1-2.5 %) as gas velocity is changed. For this case and in general terms for all the frequencies, the sound level pressure increase as superficial gas velocity becomes greater.



**Figure 7:** Sound pressure level as a function of distance for a fluidized bed filled with 600-1000 ground walnut shell for different  $U_{mf}$  values

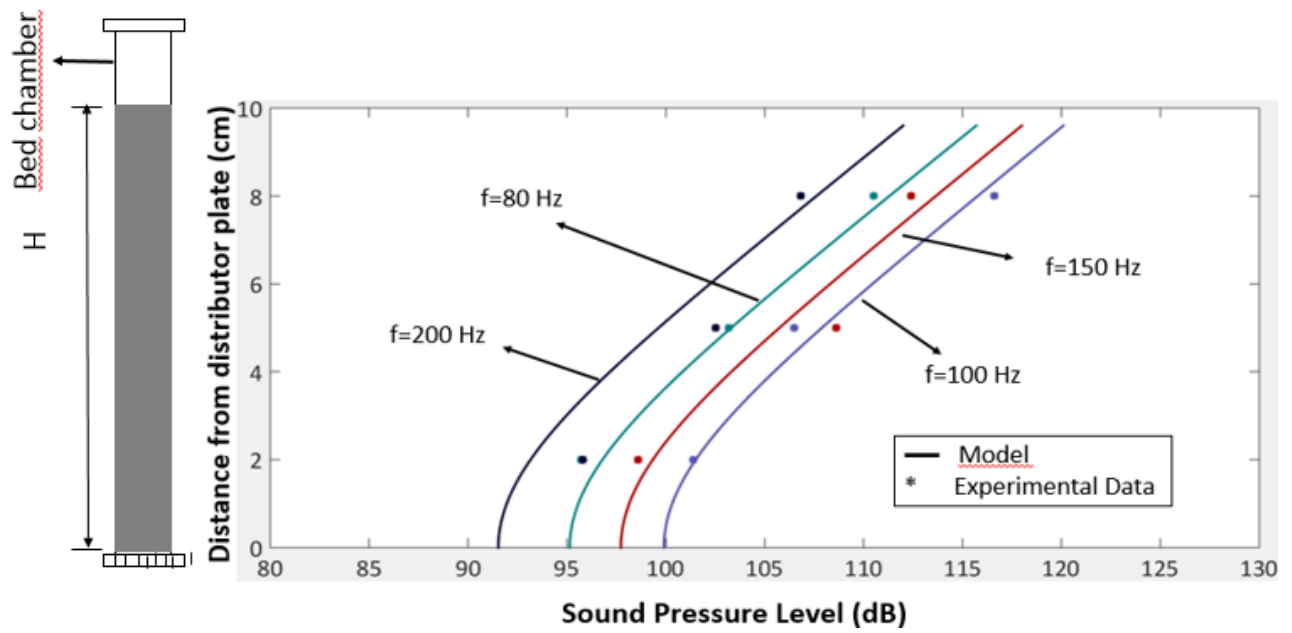
## 2.2 Comparison between model and experimental results:

Figure 8 shows the relation between experimental and modelling data for sound pressure level distribution as a function of distance from the distributor plate for an empty reactor. The model shows a good agreement with the experiments in exception of the profile for a frequency of 100 Hz. This is due to this wave frequency is close to the natural frequency of the fluidized bed (103.5 Hz) which was obtained applying Eq (7) and also to the loudspeaker natural frequency. This effect is due to the natural frequency predicted by the model assumes that the bed and top chamber have the same acoustic impedances (are made of the same material) and do not include the interactions of reflected waves from the walls of the cylinders.



**Figure 8:** Experimental and model data for sound pressure level as a function of distance from the distributor plate for an empty reactor

Furthermore, as shown in Fig 9, when material is added the model include the effect of attenuation which was calculated using Eq (15) for each frequency using the experimental data and taking as a reference point the theoretical approach for obtaining this coefficient by Eq (13). Figure 9 shows experimental and model sound level pressure comparison as a function of distance from the distributor for glass beads. The model shows a good agreement with the experiments.



**Figure 9:** Experimental and model data for sound pressure level as a function of distance for 300-600  $\mu\text{m}$  glass beads fluidized bed

## CONCLUSION

The acoustic level distributions inside the bed and top chamber of a fluidized bed for an empty reactor exhibits a standing acoustic wave behavior. The results showed that increasing the superficial gas velocity a slight change in the sound pressure level profile was produced, in general terms increasing the superficial gas velocity generates an increment in the sound intensity.

Moreover, when material is added to the bed chamber the sound pressure level pattern is modified. The acoustic intensity is decreased by the effect of attenuation as it propagates deeper in the solid due to part of the wave energy is transmitted downward to the material on the other is reflected back to the freeboard region.

The model developed shows a good agreement with the experiments results for an empty reactor and a bed filled with glass beads (300-600  $\mu\text{m}$ ). The deviations could be produced by the noise of the room and due to the Microphone Measurement device used was omnidirectional and the sound intensity could be affected by the wave reflected from the bed wall.

## REFERENCES

- Cocco, R., Karri, S. B. R., & Knowlton, T. (2014). Introduction to fluidization. *Chemical Engineering Progress*, 110(11), 21–29.
- Crowe, C. T., & Michaelides, E. E. (2006). *Basics Concepts and Definitions. Multiphase Flow Handbook*.
- Escudero, D. (2014). Characterization of the Hydrodynamic Structure of a 3D Acoustic Fluidized Bed.
- Escudero, D., & Heindel, T. J. (2013). Minimum fluidization velocity in a 3D fluidized bed modified with an acoustic field. *Chemical Engineering Journal*, 231, 68–75.  
<http://doi.org/10.1016/j.cej.2013.07.011>
- Geldart, D. (1973). Types of gas fluidization. *Powder Technology*. 7(5): 285-292.
- Guo, Q., Liu, H., Shen, W., Yan, X., & Jia, R. (2006). Influence of sound wave characteristics on fluidization behaviors of ultrafine particles. *Chemical Engineering Journal*, 119(1), 1–9. <http://doi.org/10.1016/j.cej.2006.02.012>
- Guo, Q., Zhang, J., & Hao, J. (2011). Flow characteristics in an acoustic bubbling fluidized bed at high temperature. *Chemical Engineering and Processing: Process Intensification*, 50(3), 331–337. <http://doi.org/10.1016/j.cep.2010.10.003>
- Herrera, C. A., Levy, E. K., & Ochs, J. (2002). Characteristics of acoustic standing waves in fluidized beds. *AIChE Journal*, 48(3), 503–513. <http://doi.org/10.1002/aic.690480309>
- Kaliyaperumal, S., Barghi, S., Zhu, J., Briens, L., & Rohani, S. (2011). Effects of acoustic vibration on nano and sub-micron powders fluidization. *Powder Technology*, 210(2), 143–149. <http://doi.org/10.1016/j.powtec.2011.03.007>
- Kinsler, L. et al. (2000). *Fundamentals of Acoustics*. John Wiley & Sons.
- Levy, E. K., Shnitzer, I., Masaki, T., & Salmento, J. (1997). Effect of an acoustic field on

bubbling in a gas fluidized bed. *Powder Technology*, 90(1), 53–57.

[http://doi.org/10.1016/S0032-5910\(96\)03199-3](http://doi.org/10.1016/S0032-5910(96)03199-3)

Ramos Caicedo, G., García Ruiz, M., Prieto Marqués, J. J., & Guardiola Soler, J. (2002).

Minimum fluidization velocities for gas-solid 2D beds. *Chemical Engineering and Processing*, 41(9), 761–764. [http://doi.org/10.1016/S0255-2701\(02\)00005-3](http://doi.org/10.1016/S0255-2701(02)00005-3)

Reynolds, D. D. (1988). Engineering Principles of acoustics noise and vibration control, 48(2), 307–325.

Russo, P., Chirone, R., Massimilla, L., & Russo, S. (1995). The influence of the frequency of acoustic waves on sound-assisted fluidization of beds of fine particles. *Powder Technology*, 82(3), 219–230. [http://doi.org/10.1016/0032-5910\(94\)02931-D](http://doi.org/10.1016/0032-5910(94)02931-D)

Shuai, W., Xiang, L., Huilin, L., Guodong, L., Jiaying, W., & Pengfei, X. (2011). Simulation of cohesive particle motion in a sound-assisted fluidized bed. *Powder Technology*, 207(1-3), 65–77. <http://doi.org/10.1016/j.powtec.2010.10.011>

Xu, C., Cheng, Y., & Zhu, J. (2006). Fluidization of fine particles in a sound field and identification of group C/A particles using acoustic waves. *Powder Technology*, 161(3), 227–234. <http://doi.org/10.1016/j.powtec.2005.11.005>

## ANEXO A: SOUND PRESSURE LEVEL DEFINITION

Sound pressure level is defined as the amplitude of the acoustic pressure in a logarithm scale and defined as the threshold of hearing. It is measured in dB and it is expressed by the following equation:

$$SPL = 20 \log \left( \frac{P_{rms}}{P_{ref}} \right) \quad (17)$$

where SPL is the sound pressure level in dB,  $P_{ref}$  is the sound pressure reference of the human threshold of hearing equal to  $2 \times 10^{-5}$  Pa and  $P_{rms}$  is the root mean square pressure defined by:

$$P_{rms} = \frac{|p(x, t)|}{\sqrt{2}} \quad (18)$$

where  $|p(x, t)|$  is the absolute sound pressure in Pa.